Fluid Dynamics Research 5 (1990) 337–350
North-Holland

Refraction of a shock wave at an air–water interface *

L.F. HENDERSON

Department of Mechanical Engineering, University of Sydney, Australia

Jia-Huan MA

Institute of Mechanics, Chinese Academy of Science, Beijing, China

Akira SAKURAI

Department of Mathematical Sciences, Tokyo Denki University, Japan

and

Kazuyoshi TAKAYAMA

Institute of Fluid Science, Tohoku University, Sendai, Japan

Received 14 February 1989

Abstract. The problem of a shock wave refracting at an air/water interface is considered as an example of a typical refraction of a shock passing from a medium of lower impedance to one of substantially higher impedance. Relatively little work on the subject has been reported in the open literature. This may be due to the fact that only a small amount of the energy associated with the shock in the air enters the water, so there is not much engineering interest in the effects in the water. In spite of this, there are some interesting phenomena. This paper reports on experiments on a plane air–water interface in a shock tube, together with associated numerical studies using the TVD method. Excellent agreement was obtained. Application to a height-of-burst explosion in air over water is also reported. In this case the experiments were done with small lead azide charges. This work was supported by analytical studies from which an unexpected result was reported: that the pressure tended to increase with water depth. There was some experimental evidence to support this result.

1. Introduction

Consider a shock wave propagating in a medium of comparatively low density, such as a gas, and then impinging on a second medium of much greater density, such as a liquid. The shock will be refracted (bent) as it passes from one medium to the other. In should be noted that the phenomena of reflection which appear with various gas–liquid combinations have some features in common. This is due essentially to the fact that the reflection in this case is somewhat similar to that of a shock in a gas reflecting off a rigid surface. More precisely, this general similarity is caused by the large difference in the shock impedance between the two media. For example, when a shock passes from air into water the impedance of the water is about three orders of magnitude greater than that of the air; so compared with air, water is an

* Based on discussions at the "2nd Workshop on Shock Waves", August 17–18, 1988, at University of Sydney.

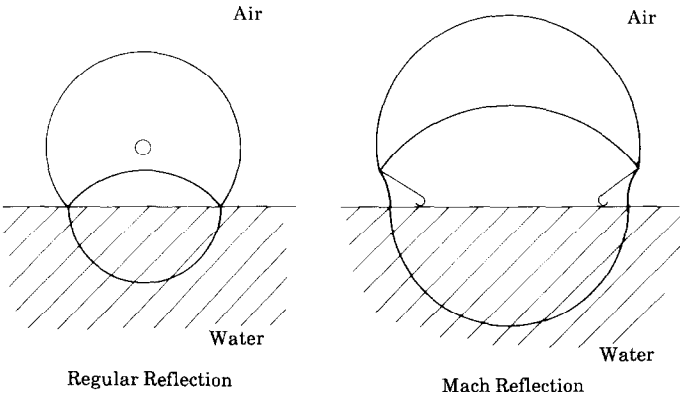

Fig. 1. Illustration of air–water refraction in connection with height-of-burst problem in air above an ocean, showing the change in the nature of refraction from regular to irregular (after Flores and Holt, 1982).

almost rigid body. This implies that very little energy will be transmitted from the air to the water: most of it will be reflected back into the air by the refraction.

There is comparatively little work in the open literature about the problem. Von Neumann (1943) considered shocks in gases and in water-like substances but did not discuss the air–water refraction. Polachek and Seeger (1951) did consider some refraction problems and attempted to construct a definition of shock impedance, but this has been criticized recently (Henderson, 1988). Flores and Holt (1982) studied air–water refraction and also the reciprocal case, water–air. They considered, in connection with height-of-burst problems in air above an ocean, ranges of angles of incidence of the shocks from normal to critical and beyond. The nature of the refraction changes from regular to irregular (fig. 1) when the critical angle is exceeded (Jahn, 1956; Abdel-Fattah et al., 1976; Abdel-Fattah and Henderson, 1978). Their analysis was based on the one-dimensional Rankine–Hugoniot equations, the perfect gas equation of state for air, and the modified Tait equation of state for water, namely,

$$P = B(s)[(\rho/\bar{\rho})^{\gamma} - 1], \tag{1}$$

where P is the pressure downstream of the shock, $B(s) \approx 3 \times 10^8$ Pa is a slowly varying function of the entropy s, γ is a constant usually taken to be $\gamma = 7.15$, although they used $\gamma = 7$, and $\bar{\rho}$ is a reference density.

There may be two reasons why so little work has appeared in the literature. One is of course that since only a small fraction of energy is transmitted into the water, there is not much engineering interest in the effects – the energy transfer is very inefficient. Another reason that the diversity of the phenomena makes it difficult to establish common properties, especially to the features on the liquid side. Nevertheless, the known effects can be of interest in their own right. For example, although little energy is transmitted, the shock intensity can increase substantially in water, and similarly in numerous other gas–liquid shock refractions. It is stressed in this connection that the small energy fraction can be utilized as an assumption for approximation in the analytical approach for the details of the flow field, although the overall nonlinear nature of the problem cannot be disregarded.

In the present paper, some general properties of the refraction are considered in section 2, and then special cases are considered in later sections: for example, self-similar shocks in section 3, the air–water refraction of a plane shock in section 4, and the water wave induced by a height-of-burst in air in section 5. The complexity of the phenomena makes it necessary to consider the special cases in this way.

2. General properties of refraction

2.1. The relative refractive index and the wave impedance

These properties are conveniently described in terms of the relative refractive index n of the two media, and the shock impedances Z_i and Z_t of each of the media. The definitions are those given by Henderson (1988) for n,

$$n \equiv |U_i|/|U_t|, \tag{2}$$

where U_i and U_t are the velocities of the shock in the initial and in the receiving media, respectively. It will be shown below that n is a measure of the capacity of the two media to refract (deflect) the incident wave. The refraction is said to be slow–fast when $n < 1$, for example from air into water, and conversely fast–slow when $n > 1$, as from water into air. However, there is no refraction when $n = 1$, even if the media differ in composition or in state.

The wave impedance Z is defined in general terms as the stress (pressure) which must be applied to a compressible substance in order to induce a particle flow in it of unit velocity. For the incident wave i, this gives

$$Z_i \equiv \frac{P_1 - P_0}{U_{pi}} = \frac{P_1 - P_0}{u_1 - u_0}, \tag{3}$$

where P is the pressure and the subscripts 0, 1 refer to conditions upstream and downstream of i; U_{pi} is the driving piston velocity, that is, the velocity of the perturbing boundary or other disturbance which generates i, and u is the particle velocity of the medium. It is also possible to rewrite Z_i entirely in terms of the variables of state by the use of the one-dimensional equations of continuity and momentum. The result is

$$Z_i = \pm\left(-\frac{P_1 - P_0}{v_1 - v_0}\right)^{1/2}, \tag{4}$$

where $v = 1/\rho$ is the specific volume. Eq. (4) is valid for any Rayleigh process and for a material with an arbitrary equation of state, for example,

$$P = P(s, v), \tag{5}$$

where s is the specific entropy. Eq. (4) shows that Z is like an average adiabatic bulk modulus and, furthermore, since a Rayleigh process falls on a straight line in the (P, v) plane, eq. (4) shows also that $-Z^2$ is the slope of that line. Again, using continuity and momentum, Z_i can in addition be written as

$$Z_i = \pm\rho_0 u_0, \tag{6}$$

$$Z_i = \pm\rho_1 u_1. \tag{7}$$

If one takes coordinates which are at rest with respect to the incident wave, then it follows that

$$U_i = -u_0. \tag{8}$$

Now at the acoustic limit $u_i \to a_0$, where a_0 is the velocity of sound, and by eqs. (6) and (8), $Z_i \to \mp\rho_0 a_0 \equiv Z_a$, which is the acoustic impedance, as it should. Eq. (6) can also be written as

$$Z_i = \mp\rho_0 U_i, \tag{9}$$

and because U_i depends on U_{pi}, Z_i is a function not only of the variables of state (ρ_0, $a_0(T_0)$) but also of the perturbing boundary parameter U_{pi}. This means that Z_i is amplitude-dependent, while by contrast the acoustic impedance is independent of U_{pi} and depends only on the state

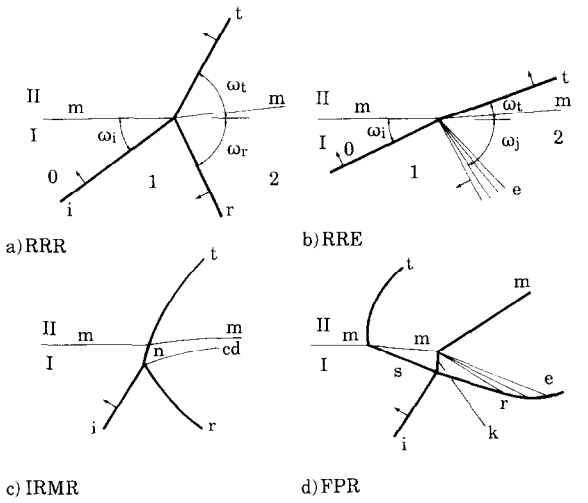

Fig. 2. Typical regular and irregular shock wave refraction systems. (a) Regular refraction with a reflected shock wave, r, RRR. (b) Regular refraction with a reflected expansion wave, e, RRE. (c) Irregular refraction with a Mach reflection, IRMR. (d) Irregular refraction with a free precursor shock system ts, FPR, i, incident shock; t, transmitted shock; r, reflected shock; e, expansion wave; n, Mach shock; ts, transmitted and side shock precursor shocks; k, modified shock; mm, media interface; I, incident medium, II, transmitting medium; ω_i, angle of incidence; ω_r, angle of reflection; ω_t, angle of transmission.

variables. This feature of Z_i is to be expected of course since i is in general a non-linear wave.

2.2. *The reflection and transmission coefficients*

Referring to figs. 2 and 3, the pressure intensity coefficients R and T are defined as

$$R \equiv \frac{P_2 - P_1}{P_1 - P_0}, \tag{10}$$

$$T \equiv \frac{P_t - P_0}{P_1 - P_0}. \tag{11}$$

The wave intensity I is the average power through unit area normal to the direction of propagation. Then,

$$I_i \equiv (P_1 - P_0)U_{pi} = (P_1 - P_0)(u_1 - u_0), \tag{12}$$

with similar expressions for the transmitted and reflected waves. Using eq. (3),

$$I_i = \pm \frac{(P_1 - P_0)^2}{|Z_i|}, \tag{13}$$

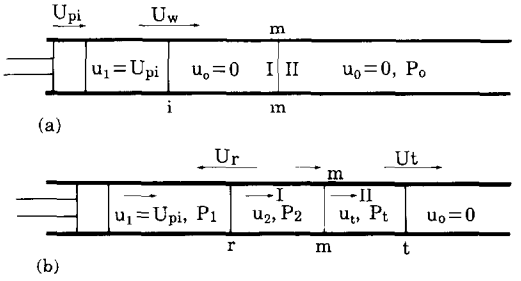

Fig. 3. Refraction of a normal shock wave at head-on incidence.

and again also for the other waves. The intensity coefficients R_I and T_I may now be defined as follows:

$$R_I \equiv \frac{I_r}{I_i} = \left| \frac{(P_2 - P_1)^2}{(P_1 - P_0)^2} \frac{Z_i}{Z_r} \right| = R^2 \left| \frac{Z_i}{Z_r} \right|, \tag{14}$$

$$T_I \equiv \frac{I_t}{I_i} = \left| \frac{(P_t - P_0)^2}{(P_1 - P_0)^2} \frac{Z_i}{Z_t} \right| = T^2 \left| \frac{Z_i}{Z_t} \right|. \tag{15}$$

The power transmitted along a streamtube of cross-sectional area A is AI; therefore the power coefficients R_π and T_π are

$$R_\pi \equiv \frac{A_r}{A_i} \frac{I_r}{I_i} = \frac{A_r}{A_i} R^2 \left| \frac{Z_i}{Z_r} \right|, \tag{16}$$

$$T_n \equiv \frac{A_t}{A_i} \frac{I_t}{I_i} = \frac{A_t}{A_i} T^2 \left| \frac{Z_i}{Z_t} \right|. \tag{17}$$

2.3. *The interface boundary conditions*

Again referring to figs. 2 and 3, it will be assumed that everywhere across the interface between the media the pressure is continuous and so also is the component of the particle velocity u perpendicular to the interface. Hence,

$$P_t = P_2, \tag{18}$$

$$u_t = u_2. \tag{19}$$

Confining attention to the normal refraction for the present (fig. 3), these equations may be more conveniently written as

$$(P_t - P_0) = (P_2 - P_1) + (P_1 - P_0), \tag{20}$$

$$(u_t - u_0) = (u_2 - u_1) + (u_1 - u_0),$$

$$\therefore \quad U_{pt} = U_{pr} + U_{pi}, \tag{21}$$

From eqs. (19) and (20) and also from eq. (3) and the similar definitions of Z_r and Z_t one may now obtain without difficulty expressions for the reflection and transmission coefficients, namely,

$$R = \frac{Z_r}{Z_i} \frac{Z_t - Z_i}{Z_r - Z_t}, \tag{22}$$

$$T = \frac{Z_t}{Z_i} \frac{Z_i - Z_r}{Z_t - Z_r}, \tag{23}$$

and similarly for R_I, T_I, R_π and T_π.

For oblique refraction, fig. 2, eq. (20) is still valid, but (21) must be modified to

$$U_{pt} \cos \beta_t = U_{pr} \cos \beta_r + U_{pi} \cos \beta_i, \tag{24}$$

where β_i, β_r, β_t, are the wave angles of i, r and t measured with respect to the *disturbed* interface. If the impedance for oblique waves is now defined as

$$Z_i \equiv \frac{P_1 - P_0}{U_{pi} \cos \beta_i}, \tag{25}$$

and similarly for Z_r, Z_t, then (22) and (23) become valid for these waves, and so do all the other coefficients.

2.4. The fundamental law of refraction

This law is applicable to oblique shock systems. If for example a regular wave refraction (fig. 2) is to retain the same structure as it propagates, then every wave in the system must have the same velocity along any straight trajectory path that passes through the junction (triple) point of the waves. This gives the law

$$U = \frac{U_i}{\sin \beta_i} = \frac{U_r}{\sin \beta_r} = \frac{U_t}{\sin \beta_t}. \tag{26}$$

Now, from eq. (6),

$$Z_i = \pm \rho_0 U_i, \quad Z_t = \pm \rho_t U_t, \tag{27}$$

and remembering that Z_t always has the same sign as Z_i,

$$\frac{Z_i}{Z_t} = \frac{\rho_0 U_i}{\rho_t U_t}, \tag{28}$$

and, combining eq. (28) with eqs. (2) and (26),

$$n \equiv \frac{U_i}{U_t} = \frac{\rho_t Z_i}{\rho_0 Z_t} = \frac{\sin \beta_i}{\sin \beta_t}, \tag{29}$$

which is the fundamental equation for oblique refraction. Thus n is seen to be a measure of the two media to bend or refract the incident wave, for when $n > 1$ $\beta_i > \beta_t$, when $n < 1$ $\beta_i < \beta_t$, and there is no refraction when $n = 1$ because then $\beta_t = \beta_i$.

One may also write

$$\cos \beta_t = \sqrt{1 - \sin^2 \beta_t}, \tag{30}$$

$$\therefore \quad \cos \beta_t = \sqrt{1 - n^{-2} \sin^2 \beta_i}, \tag{31}$$

so β_t is only real when $\beta_t \leqslant \beta_c$, where β_c, which is called the *angle of intromission*, is obtained from eq. (31) as

$$\sin \beta_c = n = \frac{|U_i|}{|U_t|}. \tag{32}$$

When $\beta_i > \beta_c$ the refraction law is violated, and the regular refraction breaks up into a free precursor shock system (fig. 2); however, this is only possible for a slow–fast refraction where $n < 1$.

2.5. The air–water interface

The acoustic impedance of air and water at a pressure of 1 atm and at 15 °C is respectively 410 and 1.5×10^6 kg m^{-2} s^{-1}. So the impedance of water is about 3500 times larger than that of the air. However, suppose there is a shock in the air which makes head-on incidence with the water surface and that the Mach number of the air shock is $M_s = 3.5$. Then, by the Tait equation (1) and the boundary condition (18) the disturbance in the water is still essentially an acoustic wave. The ratio of the acoustic impedance in the water to the *shock* impedance in the air is still about 1000. From eqs. (22) and (23) we then have approximately

$$R \approx Z_r/Z_i, \quad T \approx 1 + Z_r/Z_i. \tag{33}$$

The analysis can be taken further if it may be assumed that air is a perfect gas, for then, by the von Neumann (1943) formula for head-on reflection at a rigid surface to which the water is a good approximation, we can calculate R and T approximately,

$$R = \frac{2\gamma}{(\gamma - 1) + (\gamma + 1)P_0/P_1}, \tag{34}$$

$$T = \frac{(3\gamma - 1) + (\gamma + 1)P_0/P_1}{(\gamma - 1) + (\gamma + 1)P_0/P_1}. \tag{35}$$

Since $\gamma = 1.4$ for air and $P_0/P_1 = 0.0708$ for $M_s = 3.5$, we get $R = 4.91$ and $T = 5.91$. Thus, the pressure wave in water is of greater intensity than that of the incident shock in air, while the reflected shock is of less intensity than i. Using eqs. (14)–(17), the intensity coefficients are $R_\pi = R_i \approx R = 4.91$ and $T_\pi = T_1 = 0.0349$, so only $\approx 3.5\%$ of the energy in transmitted into the water. The same value of the energy partition has been reported also by an entirely different approach based on a surface burst model (Sakurai, 1974).

The refraction is slow–fast since $n = 341 \times 3.5/1500 = 0.796$, so the angle of intromission is $\beta_c = 52.75°$. This means that if $\beta_i < 52.75°$ the refraction will be regular, but if $\beta_i > \beta_c$ it will be irregular with a free-precursor appearing in the water. For an acoustic wave passing from air to water, $n = 341/1500 = 0.227$ and $\beta_c = 13.14°$, which demonstrates how amplitude-dependent the refraction is.

3. Self-similar refraction and viscosity

The refraction is regular when $\beta_i < \beta_c$ for the air–water interface. If the thickness of the incident shock is much smaller than its radius of curvature, then one can regard the shock as locally plane at the interface in a region which is small compared with the radius of curvature. In these circumstances there exist several situations of engineering interest where the flow near the interface and close to the waves is self-similar or nearly so. This implies of course that there is no length or time scale present in the region. The local regions are then as shown in fig. 2, and the theory of the previous section is immediately applicable to it.

Effect of viscosity: So far this effect has been ignored on the assumption that the Reynolds number for any practicable situation is likely to be large. However, at, and near, the interface there may be local viscous effects of significance. If they are to be taken into account, then the boundary conditions (20) and (24) must be supplemented by the shear conditions parallel ot the interface, that is, by

$$v_1' = v_2', \tag{36}$$

$$\mu_t \frac{\partial u_t}{\partial x} = \mu_i \frac{\partial u_2}{\partial x}, \tag{37}$$

where v_1' and v_2' are the components of the fluid particle velocities parallel to the interface, and μ_i, and μ_t are the fluid viscosities. The x axis is chosen to coincide with the *disturbed* interface. It is expected that viscosity would cause some local deviation from self-similarity.

An example of a shock refracting at an air–water interface is shown in fig. 4, which is a result of the experiment on a height-of-burst 10 mm above the water surface. The experiment was conducted at the Institute of Fluid Science, Tohoku University. A 4 mg lead azide pellet was pasted on a thin cotton thread and ignited by Q-switched laser beam (Takayama, 1989). It should be noticed that it is an irregular system similar to that in fig. 1b, and also that the shock thickness in air is much smaller than its radius of curvature. Accordingly, the assumption of self-similarity is expected to be reasonable near the surface and close to the shocks.

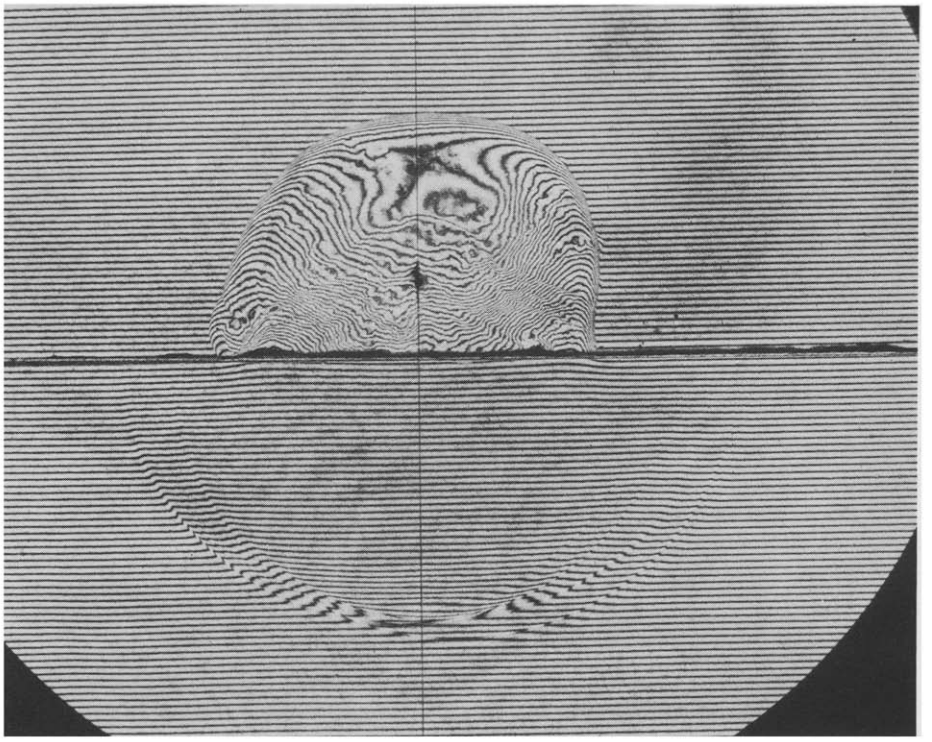

Fig. 4. Holographic interferogram of explosion of a 4 mg lead azide pellet 10 mm above the water surface, for illustration see fig. 8b.

Now, the angle of incidence ω_i of the air shock front can be measured from the photograph as $\omega_i = 64.6°$, and the initial shock pressure value there can also be estimated from the measurement of the radius of spherical air blast and the pressure distance relation (Kinney, 1962), from which the shock Mach number there was found to be $M_s = 1.37$. The angle of intromission was then $\beta_c = 18.8°$, so the system was an irregular refraction. The precursor wave in water was far ahead of the incident wave.

4. A plane shock refracting at an air–water interface

4.1. Tilted shock tube experiment

The experiments were conducted in a tilted shock tube of the Institute of Fluid Science, Tohoku University. The shock tube consisted of a low-pressure channel 30 mm × 40 mm in cross section and 3 m long and a high-pressure chamber 50 mm in diameter and 2 m long. The low-pressure channel was connected to a test section, as shown in fig. 5. The whole shock tube could be tilted with the center of rotation at the test section. The "water wedge" was established by first tilting the shock tube to the desired angle θ and then introducing the water into its test section. The water wedge angle was of course determined by θ (fig. 5). The surface tension contact angle could be adjusted by the filling procedure and by the evacuation of the tube.

The flow was visualized with the help of double exposure holographic interferometry. It was based on shadowgraph or schlieren technique. The detailed arrangement of the optical

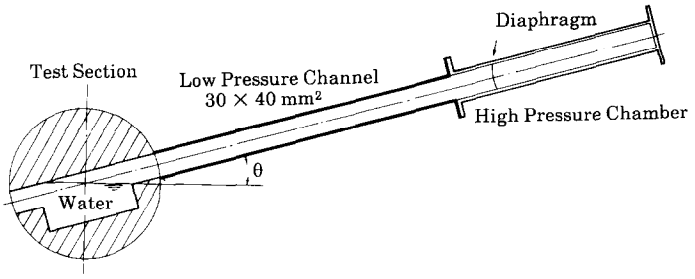

Fig. 5. Arrangement of tilted shock tube.

equipment has been described elsewhere (Takayama, 1983). The light source was a ruby laser (Apollo lasers Inc. 22HD, 2 J/pulse, ≈ 30 ns pulse duration). The first exposure was made before the event and the second one was triggered by the event itself. Since in holographic interferometry the fringes are generated by phase changes to the light beams between the two exposures, the non-uniformity fo the test medium did not significantly affect the production of the fringes. When the time interval between the two exposures was a little longer, a fringe could be observed in the water. This was attributed to the natural convection in the water and it could be readily distinguished from the fringes generated by the dynamic effect. It should be emphasized that double exposure holographic interferometry *is* successful for the study of shock refraction at a gas–liquid interface.

Typical interferograms are shown in figs. 6a and 6b. In fig. 6a, the phenomenon is an irregular system containing a Mach reflection with an angle of incidence $\omega_i = 30°$. In fig. 6b it is an apparent regular system with $\omega_i = 53.3°$, and in both cases the Mach number of the incident shock is $M_s = 1.79$. Now the angle of intromission β_c is 24°, so paradoxically *both* of these refractions are irregular. In figs. 6a and 6b, there is a fringe visible in front of the incident shock and in the water phase. This is a free precursor acoustic wave front. However this wave is so weak that it has negligible effect on the air–water interface in front of the incident shock wave. Therefore we may neglect the effect that the acoustic free precursor has on the gas phase and the systems in that phase can be treated either as an irregular (Mach) reflection as in fig. 6a, or as a regular reflection as in fig. 6b. This of course resolves the paradox. In both cases the liquid surface is effectively rigid, and in fact it will be shown below that the deformation of the liquid surface was less than 0.03 mm. It should be noted that for fig. 6 one fringe shift in water corresponds to 6.3×10^{-3}% of the water density at standard conditions.

4.2. Numerical simulation

The numerical studies of the above phenomenon were carried out with the help of TVD (total variation diminishing) finite difference scheme which was applied to the Navier–Stokes equations. This scheme is successful for solving shock flow problems with complicated boundary conditions. The full Navier–Stokes equations were utilized for the gas phase, while for the liquid phase the Euler equations were used with the Tait equation of state instead of the energy conservation equation. This calculation automatically assumed that the flow in the water phase was homotropic. The shock Mach number range in the water in the present study was rather close to unity, so the assumption of homotropic water phase was reasonable. The boundary conditions at the gas–liquid interface was as follows: the pressure, velocity components, and shear stress were continuous, as given by eqs. (36) and (37), and there was no deformation at the gas–liquid interface. Later, by integrating the component of the velocity normal to the interface, the deformation of the interface was evaluated and found to be at most

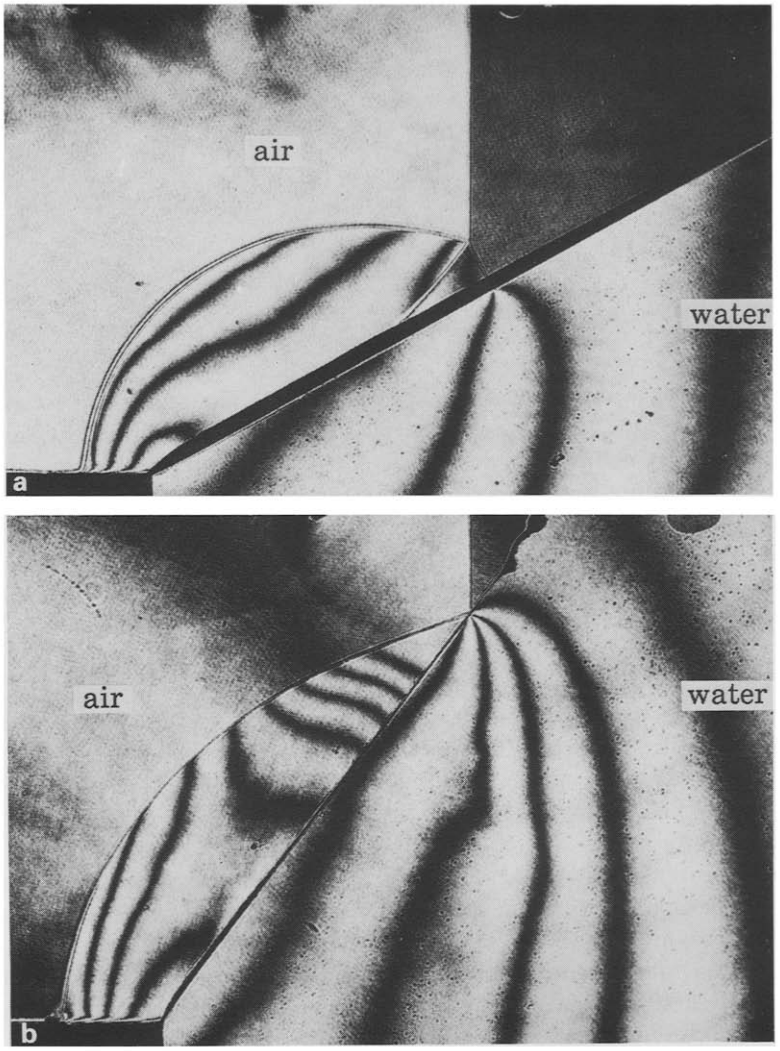

Fig. 6. Interferograms of shock reflection over water surface, $M_s = 1.79$. (a) Mach reflection, $\theta_w = 30.0°$, (b) regular reflection, $\theta_w = 53.3°$.

0.03 mm near the corner where the liquid surface met the shock tube bottom wall. Therefore the assumption of a non-deformable boundary seems acceptable. The mesh numbers were 250×150 in the gas phase and also 250×150 in the liquid phase. Finer mesh distributions were used near the gas–liquid boundary where there are at least 15 meshes in the boundary layer.

Some of the computed results are shown in figs. 7a and 7b, which correspond to the interferograms in figs. 6a and 6b, respectively. Figs. 7a and 7b show the isopycnics. Good agreement can be seen between figs. 6 and 7 (Miyoshi, 1988).

5. The water disturbance induced by a height-of-burst in air

We will consider the disturbance induced in the water by an air blast at a height h above the surface. The problem is illustrated in fig. 8, and a photograph of such a burst is shown in fig. 4.

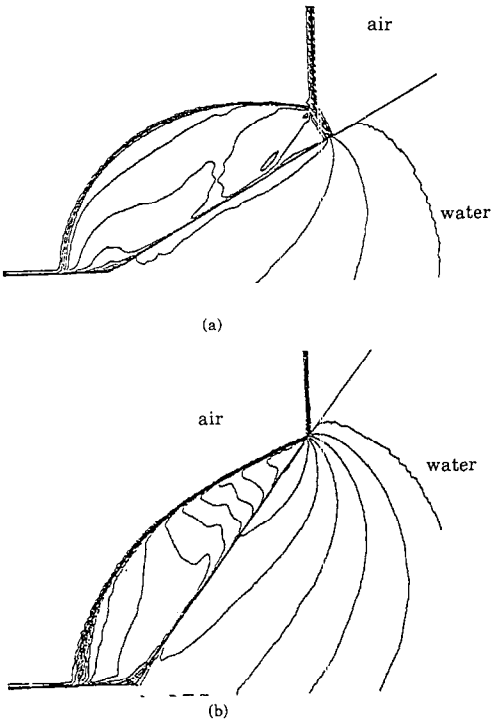

Fig. 7. Density distribution. Results of numerical simulation, $M_s = 1.79$. (a) Mach reflection, $\theta_w = 30.0°$, (b) regular reflection, $\theta_w = 53.3°$.

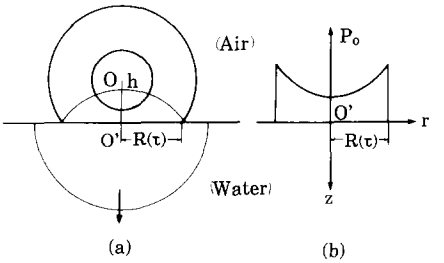

Fig. 8. Airblast-induced water shock wave. (a) Shock front geometries, (b) Illustration of airblast loading on the water surface.

The objective is to determine the pressure field in the water associated with the propagation of the wave in it.

A proper understanding of the problem requires both analytical and experimental approaches. The experiment shown in fig. 4 was on a small scale, and was described in section 3. The density changes in the water are usually so small that it is difficult to determine the density field accurately, although some pressure measurements have been reported by Sakurai and Pinkston (1967). There is a similar problem with the theory which makes purely numerical simulation difficult, especially since this must be combined with the large impedance mismatch at the interface. Here we use the analytical approach with a proper mathematical model. It is based upon two assumptions:

(a) The pressure at the water surface is closely approximated by the reflection of the air blast at a plane rigid surface.

(b) The pressure changes in the water are so small that they can be closely approximated by an acoustic field. Actually the Tait equation of state (1) indicates that the pressure needs to be more than about 1500 atm before non-linear effects become significant.

These assumptions are a great simplication of the theory, for we can treat the water pressure field by linear acoustics, while preserving the essential non-linear character of the phenomena in the air blast. The two effects can be largely treated separately and then patched together.

This model may be inadequate as h becomes small. However, even in this case a simple modification may suffice to recover it. It is noted also that an entirely different model is needed for the surface burst (Sakurai, 1970), and this must also be used when h becomes very small.

Thus by assumption the pressure field $P(r, z, \tau)$ in the water at point (r, z) (fig. 8) at time τ satisfies the acoustic equation

$$\frac{\partial^2 P}{\partial \tau^2} = c^2 \, \Delta P, \quad z > 0, \quad r > 0, \tag{38}$$

where c is the velocity of sound in water and τ is the time measured from the instant when the air blast first hits the water. The problem is subject to the boundary conditions

$$P(r, z, 0) = \left(\frac{\partial P}{\partial \tau} \right)_{\tau = 0} = 0, \tag{39a}$$

$$P(r, 0, \tau) = P_0(r, \tau) H(R(\tau) - r), \tag{39b}$$

$$P(\infty, \infty, \tau) = 0, \tag{39c}$$

where $R(\tau)$ is the radius of the domain on the surface $z = 0$ which is influenced by the air blast (fig. 8), $P_0(r, \tau)$ is the pressure in the domain, and H is the Heaviside function.

A solution of the system can be given in the following form:

$$P(r, z, \tau) = -\frac{1}{\pi} \frac{\partial}{\partial z} \int_{-\infty}^{\infty} \int_{-\infty}^{\infty} \frac{P(r', 0, \tau')}{\beta} \mathrm{d}x' \, \mathrm{d}y', \tag{40}$$

where

$$\beta^2 = (x - x')^2 + (y - y')^2 + z^2, \quad x'^2 + y'^2 = r'^2,$$
$$x^2 + y^2 = r^2, \quad \tau' = \tau - \beta / c,$$

and with (x, y) or (x', y') the x, y coordinates on the $z = 0$ plane.

Now the value of the peak pressure $P(0, z, z/c)$ directly under the explosion can be found exactly from the above formulas by taking the limits as $r \to 0$, $\tau \to z/c$, as

$$P(0, z, z/c) = P_0(0, 0) \left(1 + \frac{cz}{hU_h} \right)^{-1}, \tag{41}$$

where U_h is the velocity of the shock front of the free air blast at the origin $(r, z = 0)$. Since $P_0(0, 0)$ is the pressure behind the normally reflected shock it can be determined exactly with the help of the general formula (34). Its value is usually substantially higher than that of the incident wave, so the pressure in the water may be much higher than the pressure outside the water. This illustrates a fact referred to earlier, that a large impedance mismatch can lead on some occasions to a high-intensity pressure field even though only a small fraction of the energy is being transmitted.

Although it is impossible to obtain a general closed-form expression for $P(r, z, \tau)$, a very good approximation can be obtained by postulating that the input pressure $P_0(r, \tau)$ on the surface has the form

$$\begin{aligned} P_0(r, \tau) &= a_0(\tau) + r^2 a_1(\tau) + r^4 a_2(\tau) + \ldots, \quad && R \geqslant r > 0, \\ &= 0, && r > R. \end{aligned} \tag{42}$$

This makes it possible to reduce the double integral to a sum of single ones, and we get, in general,

$$P(r, z, \tau) = P_0(r, \tau - z/c) H[R(\tau - z/c) - r] + \sum_{n=0}^{\infty} \int_{\tau_1(r, z, \tau)}^{\tau_2(r, z, \tau)} f_n(r, z, \tau, \tau') a_n(\tau') \, \mathrm{d}\tau', \tag{43}$$

where the τ_1, τ_2 values and the functions f_n are determined for a given set of values of $(r, z, \tau,$

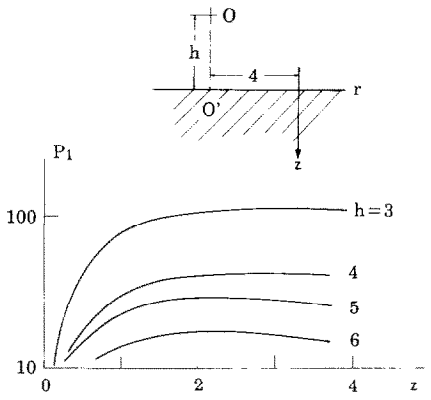

Fig. 9. Computed peak pressure values $P_1(r, z)$ versus water depth z along $r = 4$ for various heights of burst h.

τ'). Also the $a_n(\tau)$ functions are determined by the pressure behind the reflected shock wave. In practice sufficient accuracy is obtained from $a_0(\tau)$, or at most with $a_0(\tau)$ and $a_1(\tau)$. An example of the numerical results is displayed in fig. 9 for peak pressures off the center line. It has the interesting and unexpected property that the pressure is larger at greater depths. There is some experimental evidence to support this result (Sakurai and Pinkston, 1967).

6. Conclusions

The large difference in the shock impedance between a gas, such as air, and a liquid such as water means that refraction at a gas–liquid interface has the same features in common with shock reflection; the impedance mismatch between air and water is about three orders of magnitude.

Some general properties of refraction could be formulated by considering a plane shock wave refracting at an arbitrary angle of incidence at an arbitrary media interface. These properties included the refractive index, n, and the wave impedance Z_i, Z_r, Z_t, etc. of the media, and also included the law of refraction. The general properties determine the capacity of the media to refract (bend) the wave (n), the nature of the wave systems which appear – for example, regular/irregular (n, Z), and the intensity of the transmitted wave and its associated energy and power fluxes (Z).

Experimental and numerical studies were made of a less general refraction, that is, of an oblique shock wave refracting from air into water. The experiments were done with the help of a tilting shock tube and numerical work with the TVD code. The excellent agreement between the results indicates the usefulness of the code for refraction for large impedance mismatch.

Finally, and as an application, the refraction of a blast wave from a height-of-burst explosion over water was studied both analytically and experimentally. The experiments were done with small lead azide charges. The mathematical model exploited the large impedance mismatch between the media. It produced the unexpected result that the pressure in the water tended to increase with depth. There was some experimental evidence to support this conclusion.

References

Abdel-Fattah, A.M., L.F. Henderson and A. Lozzi (1976) Precursor shock waves at a slow–fast gas interface, *J. Fluid Mech. 76*, 157–176.

Abdel-Fattah, A.M. and L.F. Henderson (1978) Shock waves at a fast–slow interface, *J. Fluid Mech. 86*, 15–32.

Flores, J. and M. Holt (1982) Shock wave interactions with the ocean surface, *Phys. Fluids 25*, 238–246.

Henderson, L.F. (1988) On the refraction of shock waves, *J. Fluid Mech. 198*, 365–386.

Jahn, R.G. (1956) The refraction of shock waves at a gaseous interface, *J. Fluid Mech. 1*, 457–489.

Kinney, G.F. (1962) *Explosive Shocks in Air* (MacMillan, New York).

Miyoshi, H. (1988) Master Thesis, Graduate School of Tohoku University.

Polachek, H. and R.J. Seeger (1951) On shock wave phenomena; refraction of shock waves at a gaseous interface, *Phys. Rev. 84*, 922–929.

Sakurai, A. and J.M. Pinkston (1967) Water shock waves resulting from explosions above an air–water interface; Report 1, Results of a theoretical investigation, *Waterways Experiment Station Technical Rep. 1-777*.

Sakurai, A. (1970) A realistic approach for describing the explosion generated axi-symmetric wave propagating in a half-space, *Proc. 5th Int. Symp. Detonation* (U.S. Govt. Printing Office, Washington) p. 493.

Sakurai, A. (1974) Blast wave from a plane source at an interface, *J. Phys. Soc. Japan 36*, 610.

Sakuari, A. (1983) Blast wave – its science and engineering, *Proc. 9th Canadian Congress of Applied Mechanics*, pp. 75–83.

Takayama, K. (1983) Application of holographic interferometry to shock wave research, *Proc. of SPIE Symposium, Industrial Applications of Laser Technology, Vol. 398*, Geneva, April, pp. 174–180.

Takayama, K. (1989) Interaction of a spherical shock wave with a liquid surface, *Rep. Inst. Fluid Sci.*, Tohoku Univ. (to be published).

Von Neumann, J. (1943) Oblique reflection of shock waves, in: *Collected Works, Vol. 6* (Pergamon, Oxford) pp. 238–299.